CHAPTER 179

Two-Phase Flow Model on Oscillatory Sheet-Flow

Toshiyuki Asano

1.INTRODUCTION

Under stormy waves on a sandy beach, a flat movable bed may appear when ripples have been washed out. Studies of the sheet flow have recently received much attention because a large amount of sand is transported under such conditions. However, most of the existing studies on the sediment transport are dealing with the phenomena under small tractive forces because this is easily reproduced in a small wave tank. Until now, very little understanding has been obtained on the sheet flow phenomena.

The first systematic study on the sheet flow is likely the work of Horikawa et al.(1982). They measured the sediment transport velocity and sediment concentration in an oscillatory flume. The reported velocity and concentration profiles were different from existing results obtained under the condition of small amount of sediment movement. Yamashita et al.(1985) and Ahilan-Sleath(1987) performed similar experiments with light artificial particles as the sediment. These experiments have increased the understanding of sheet flows. However, difficulties in the measuring densely mixed sediment-fluid flow prevent investigating the detailed structures of the flow. In addition, the limited size of the experimental flume may cause several problems in generating idealistic conditions.

Since a numerical model has an advantage of being free from the restrictions imposed on the experiment, several models on the sheet flow have recently been proposed. Ahilan-Sleath modelled sediment-fluid mixture flow as a mono-phase flow with varying density in time and depth. Since this model ignores the sediment-fluid interaction, the accuracy is likely to decrease as the sediment concentration becomes higher.

Associate Professor, Department of Ocean Civil Engineering, Kagoshima University, 1-21-40, Kourimoto, Kagoshima, 890, JAPAN

The present paper develops a numerical model to analyze the oscillatory sheet flow. The mathematical formulation based on fluid-sediment two phase flow is performed by expanding models from a unidirectional flow(Bogardi(1974), Kobayashi-Seo(1985)) into an oscillatory flow. The developed model predicts the velocity field, properties of friction and sediment transport rate. The model is shown to describe existing experimental data for oscillatory sheet flow.

2. SOLID - FLUID MIXTURE MODEL FOR OSCILLATORY SHEET FLOW

(1) Basic assumptions and mathematical formulation

The mathematical model derived herein is based on a continuum assumption for fluid and a uniform cohesionless sediment mixture. The analysis is performed for the case of two dimensional oscillatory flow over a plane bed. Molecular diffusion and viscous stresses are assumed to be negligible compared with those due to turbulence.

The continuity equation for the fluid phase is

$$\frac{\partial}{\partial t}\rho(1-c)+\frac{\partial}{\partial x_j}\rho(1-c)u_j=0 \tag{1}$$

in which ρ: fluid density, c: volumetric concentration of sediment, and u_j : fluid velocity in the x_j direction. The continuity equation for the sediment phase is

$$\frac{\partial}{\partial t}\rho_s c+\frac{\partial}{\partial x_j}\rho_s c u_{sj}=0 \tag{2}$$

in which ρ_s : density of sediment, and u_{sj} : sediment particle velocity in the x_j direction.

The momentum equation for the fluid phase is described by

$$\frac{\partial}{\partial t}\rho(1-c)u_i+\frac{\partial}{\partial x_j}\rho(1-c)u_i u_j=-(1-c)\frac{\partial p}{\partial x_i}-\rho(1-c)g\delta_{i2}-f_i \tag{3}$$

in which p: pressure, g: gravitational acceleration, δ_{ij} : Kronecker delta, and f_i : x_i component of interaction force per unit volume between the sediment and fluid.
The momentum equation for the sediment phase is expressed by

$$\frac{\partial}{\partial t}\rho_s c u_{s,i}+\frac{\partial}{\partial x_j}\rho_s c u_{s,i}u_{s,j}=-c\frac{\partial p}{\partial x_i}+\frac{\partial \gamma_{ji}}{\partial x_j}-\rho_s c g\delta_{i2}+f_i \tag{4}$$

in which γ_{ij} : intergranular stress tensor.

(2) Simplification of the equations

In the following analysis, the x-axis is taken in the horizontal direction, and the z-axis is taken upward from the origin placed at the top of the immovable layer where the sediment transport velocity is always zero. The velocity component in the x and z directions is given by u and w, respectively. The equation for the mean quantities can be derived by first decomposing the instantaneous quantities in Eqs.(1) $\sim$ (4) into the steady, oscillatory and turbulent components, and then averaging the resultant equations with respect to time. Some simplifications are made by assuming $u \gg w, u_s \gg w_s$, and $u\overline{c'w'} \gg \overline{c'u'w'}$. For example, a fluid shear stress term which arises in the x- momentum equation is given by

$$\tau/\rho = -\{(1-c)\overline{u'w'} - u\overline{c'w'}\} \tag{5}$$

The turbulent eddy viscosity K_v and the turbulent diffusion coefficient K_c are introduced to represent the turbulent correlation terms by the mean quantities as shown by

$$\overline{c'w'} \simeq \overline{c'w'_s} = -K_c\frac{\partial c}{\partial z} \tag{6}$$

$$\overline{u'_s w'_s} \simeq \overline{u'w'} = -K_v\frac{\partial u}{\partial z} \tag{7}$$

Assuming that proximity effects among the sediment particles may be ignored and that the added mass force acting on a sediment particle is negligible as compared with the drag force, the interaction force between the sediment and fluid may be expressed as the sum of the buoyancy and drag force.

$$f_i = \rho c g \delta_{i2} + \frac{\rho}{2}C_D(\frac{\pi}{4}d^2)\frac{c}{\pi d^3/6}u_{i,r}\sqrt{u_r^2 + w_r^2} \tag{8}$$

in which $u_r = u - u_s$ and $w_r = w - w_s$ denote the relative velocities between the fluid and sediment and C_D is the drag coefficient. The interaction force in the x-direction is approximated by

$$f_x = \frac{\rho}{2}C_D(\frac{\pi}{4}d^2)\frac{c}{\pi d^3/6} \mid u_r \mid u_r \tag{9}$$

Rubey's formula is used to estimate the drag coefficient.

$$C_D = 24/Re + 2 \tag{10}$$

in which the Reynolds number is defined as $Re = u_r d/\nu$.

Although the intergranular stress resulted from the momentum transfer from solid to solid is not well understood yet even for steady flows, the constituitive equation of Savage-McKeown(1983) is adopted here as

$$\gamma_{xz}/\rho = 1.2\lambda^2\nu\partial u_s/\partial z \tag{11}$$

in which λ : the linear concentration related to c and to the maximum possible static concentration of uniform spheres c_{max}.

$$\lambda = 1/[(c_{max}/c)^{1/3} - 1] \tag{12}$$

The following dimensionless variables are introduced,

$$u = \overline{u}u_0,\ u_s = \overline{u}_s u_0,\ u_r = \overline{u}_r u_0, w = w_{f_0}\overline{w}/\sqrt{R},$$

$$w_s = w_{f_0}\overline{w}_s/\sqrt{R}, x = \frac{g\xi}{\omega^2},\ z = \sqrt{\nu/\omega}\zeta,$$

$$t = \tau/\omega, p = \rho(\frac{g}{\omega})u_0\overline{p}\ , K_c = \sqrt{\nu/\omega}u_0\overline{K}_c,$$

$$K_v = \sqrt{\nu/\omega}u_0\overline{K}_v,\ \sqrt{R} = u_0/\sqrt{\nu\omega} \tag{13}$$

in which u_0 :free stream velocity amplitude, w_{f_0} : settling velocity of a single sediment particle in pure water, ν: kinematic viscosity of the fluid, and ω :angular frequency of the oscillatory flow. The demensionless form of the continuity equation for the sediment phase is obtained from Eq.(2) as follows

$$\frac{\partial c}{\partial \tau} = -\frac{w_{f_0}}{u_0}\frac{\partial}{\partial \zeta}(c\overline{w}_s) + \sqrt{R}\frac{\partial}{\partial \zeta}\{\overline{K}_c\frac{\partial c}{\partial \zeta}\} \tag{14}$$

The dimensionless equation for the fluid phase momentum in the x-direction is given by

$$\frac{\partial}{\partial \tau}\{c^*\overline{u}\} + \frac{w_{f_0}}{u_0}\frac{\partial}{\partial \zeta}\{c^*\overline{u}\ \overline{w}\} =$$

$$\sqrt{R}\frac{\partial}{\partial \zeta}\{\overline{K}_V c^*\frac{\partial \overline{u}}{\partial \zeta} - \overline{K}_c\overline{u}\frac{\partial c}{\partial \zeta}\} - c^*\frac{\partial \overline{p}}{\partial \xi} - \frac{3}{4}R(\frac{u_0 d}{\nu})^{-1}C_D c \mid \overline{u_r} \mid \overline{u_r} \tag{15}$$

in which $c_* = 1 - c$.

The dimensionless equation for the sediment phase momentum in the x-direction is

$$\frac{\partial}{\partial \tau}\{c\overline{u}_s\} + \frac{w_{f_0}}{u_0}\frac{\partial}{\partial \zeta}\{c\overline{u}_s\overline{w}_s\} =$$

$$\sqrt{R}\frac{\partial}{\partial \zeta}\{\overline{K}_v\ c\frac{\partial \overline{u}_s}{\partial \zeta} + \overline{K}_c\overline{u}_s\frac{\partial c}{\partial \zeta}\} - \frac{1}{s}\ c\ \frac{\partial \overline{p}}{\partial \xi} + \frac{1.2}{s}\frac{\partial}{\partial \zeta}(\lambda^2\frac{\partial \overline{u}_s}{\partial \zeta})$$

$$+\frac{1}{s}\ \frac{3}{4}R(\frac{u_0 d}{\nu})^{-1}C_D\ c \mid \overline{u}_r \mid \overline{u}_r \tag{16}$$

in which $s = \rho_s/\rho$ denotes the specific density of the sediment. Adding Eq.(1) to Eq.(2) yields the following relation

$$(1 - c)\overline{w} + c\overline{w}_s = 0 \tag{17}$$

From the vertical momentum equation for the fluid phase given by Eq.(4), an equation for the pressure would be derived. From the corresponding equation for the sediment phase given by Eq.(5), an equation describing the relationship between the intergranular stress term $\partial\gamma_{zz}/\partial z$ and the fluid-sediment interaction term f_z would be derived. Since these equations are related to u, u_s, w, w_s, p and c in a highly non-linear fashion, the simultaneous differential equations are difficult to solve even numerically. Therefore, according to experimental results on the settling velocity in dense fluid-sediment mixture by Richardson et al.(1979), the vertical sediment velocity is assumed to be given by

$$w_s = w_{f0}[1 - (c/c_{max})]^n \tag{18}$$

in which n is an experimental variable, which is taken to be 2.3 in this study. The velocity for the fluid phase w can be calculated from Eq.(17) with estimated w_s. The pressure is assumed constant throughout the boundary layer.

The parameters involved in Eqs.(14), (15) and (16) are as follows:

$$s = \frac{\rho_s}{\rho}, \quad R = \frac{u_0^2}{\omega\nu}, \quad \frac{u_0^2}{gd}, \quad \frac{u_0 d}{\nu} \tag{19}$$

The variable of w_{f0}/u_0 in Eqs.(14), (15) and (16) is also expressed by the above parameters if w_{f0} is given by Rubey's formula.

The sediment transport field is conventionally divided into the following two regions: the bed load region where the sediment concentration is high and the particles are mainly supported by the intergranular stress, and the suspended load region where the sediment concentration is small and the particles are mainly supported by the fluid turbulent stress. According to the experiment of Wilson(1984), the thickness of bed load region, z_G, is given by

$$z_G = 10(\theta - \theta_{cr})d \tag{20}$$

in which θ is the Shields number and θ_{cr} is the critical Shields number. The thickness of the suspended load region, z_δ, is assumed to be equal to the turbulent oscillatory boundary layer for fixed beds. That is,

$$z_\delta = \kappa u_*/\omega \tag{21}$$

in which κ : Karman constant, and u_* : friction velocity.

In the bed load region, the mixing length may be governed by the distance among the sediment particles d/λ; whereas, in the suspended load region, the mixing length may be assumed to be the mixing length for the pure fluid flow with modifications of flow stratification. The turbulent eddy viscosity K_v may be expressed as follows

$$K_v = \kappa u_*(t)\beta(d/\lambda) : z < z_G/2$$

$$K_v = \frac{\kappa u_*(t)(z - z_G/2)}{1 + 4.7(z/L)} + \kappa u_*(t)\beta(d/\lambda\,|_{z=z_G/2}) : z \geq z_G/2 \tag{22}$$

in which $\hat{u}_*$: amplitude of the friction velocity, β : constant (here assumed to be 10), and L : Monin-Obukhov length written by

$$L = \hat{u}_*^3/(\kappa g(s-1)w_{f0}c) \tag{23}$$

According to the model of Brevik(1981), K_v is assumed to be constant for $z \geq z_G + \Delta$, in which Δ is given by

$$\Delta = 0.036\{2d(u_0/\omega)^3\}^{1/4} \tag{24}$$

Fig. 1 shows an example of the profile of the turbulent eddy viscosity.

The friction velocity amplitude $\hat{u}_*$ is estimated using the roughness height k_b based on the formula of Grant-Madsen(1982). Since the efficiency of the turbulent transfer for mass is generally different from that for momentum, K_c is not really the same as K_v. However, for lack of reliable data for oscillatory flow, K_c is assumed herein to be the same as K_v.

The boundary conditions for $\overline{u}$ and $\overline{u}_s$ are given as follows

$$\overline{u} = \overline{u}_s = 0, \quad \partial\overline{u}_s/\partial\zeta = 0 \quad : \zeta = 0$$

$$\partial\overline{u}/\partial\zeta = 0 \quad : \zeta = \overline{\delta} \tag{25}$$

Near the immovable layer where c is nearly equal to c_{max}, the intergranular stress in the vertical direction is assumed to equal the submerged weight of the sediment above it as hypothesised by Bagnold to avoid divergence of the calculated results.

$$| \, \partial\overline{u}_s/\partial z \, | \leq (s-1)g \, \tan\phi \int_z^\infty c dz \, /(1.2\lambda^2\nu) \tag{26}$$

The boundary conditions for the sediment concentration are given by

$$c = c_{max} \quad : \zeta = 0$$

$$-(w_{f_0}/u_0)\frac{1}{\sqrt{R}}c\overline{w}_s + \overline{K}_c\frac{\partial c}{\partial \zeta} = 0 \quad : \zeta = \overline{\delta} \tag{27}$$

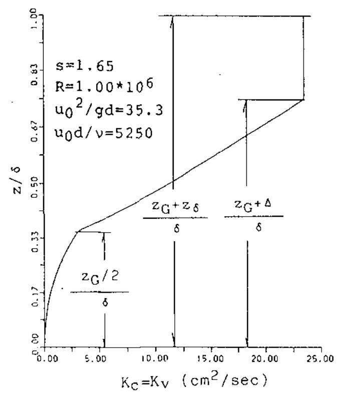

Fig. 1
Profile of turbulent eddy viscosity K_v

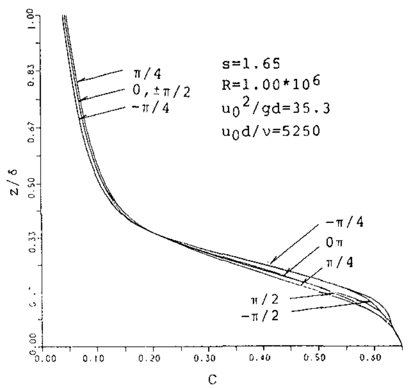

Fig. 2
Profiles of sediment concentration c

The basic equations for the numerical calculation have been obtained as Eqs.(14),(15),(16). These equations were discretized by a Crank-Nicolson implicit scheme. The number of the vertical grids was 140, and the time increment was 1/5000 of an oscillatory period. The calculation was continued until the calculated results in successive cycles converged. It was found that most of the deviation from the converged solution disappeared typically after half a period.

3. CALCULATED RESULTS

The profiles of the sediment concentration c shown in Fig.2 indicate that the concentration decreases gradually from c_{max} in the region $z/\delta \leq 0.2$, exponentially for $z/\delta \geq 0.2$.

Fig.3 shows the profiles of the fluid velocity u and the sediment transport velocity u_s. The sediment transport velocity u_s is found to be nearly zero close to the immovable layer around $z/\delta \leq 1/6$ because the intergranular stress term becomes very large in this region. The fluid motion is also suppressed due to the drag resistance between the fluid and sediment. In the region $1/6 \leq z/\delta \leq 1/3$, a phase precedence over the free stream velocity is observed. In the region $z/\delta \geq 1/3$, $| u |$ is always larger than $| u_s |$ in the accelerating phase, and smaller in the decelerating phase. This property is caused by the difference of the inertia between the sediment and fluid particles.

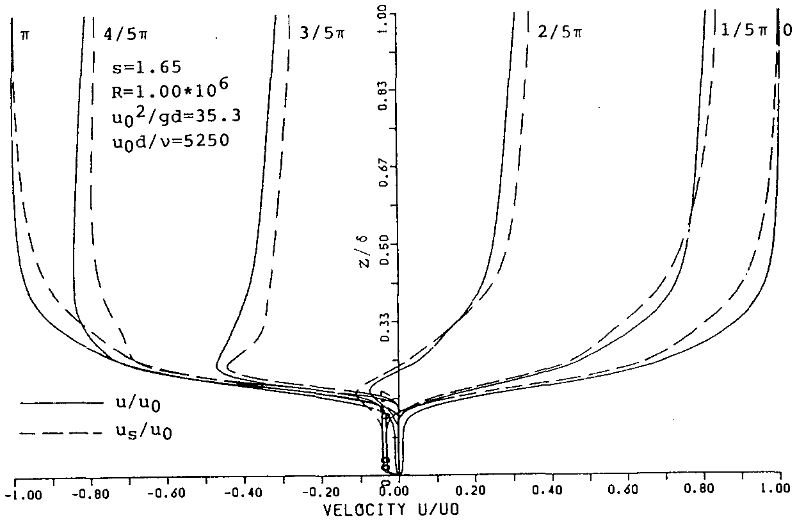

Fig. 3 Profiles of horizontal fluid velocity u (solid line) and sediment transport velocity u_s (dotted line)

The phase variation of the concentration is depicted in Fig. 4. The phase variations of the fluid velocity are given in Fig. 5. The results at $z/\delta = 0.1$ and 0.15 near the immovable layer show peculiar variations which are similar to the variations of the pressure gradient $-\partial p/\partial x$. The fluid flow around this level resembles a seepage flow because the concentration there is close to the maximum packing concentration. At $z/\delta = 0.2$, u and u_s increase gradually up to the maximum, then decrease suddenly. This result can be related to the temporal variation of the concentration.

Fig.6 is a semi-log plot of the horizontal fluid velocities at the phase = 0π for various values of the specific density s. The velocity profiles can be approximated by log-linear lines over a wide range. The intersection, z_0, of the z-axis with the extended log-linear line, which corresponds to the roughness

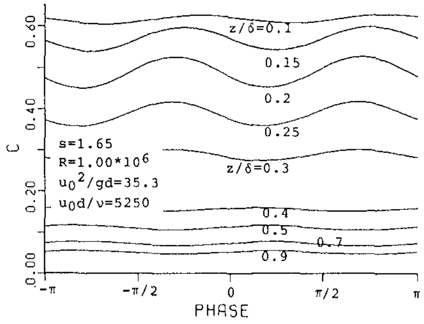

Fig. 4 Phase variation of sediment concentration

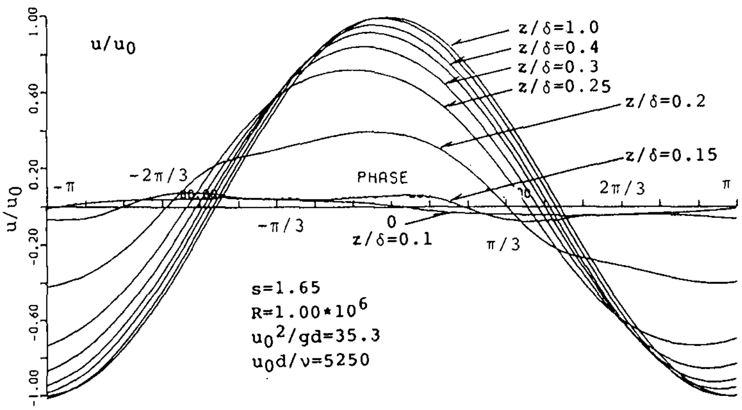

Fig. 5 Phase variation of horizontal fluid velocity

height, decreases with the increase of s. The gradient , α, of the log-linear line decreases slightly with the increase of s. The log-linear part of the velocity distribution is described by

$$u/u_0 = \alpha \ln(z/z_0) \tag{28}$$

Fig.7 (a) and (b) show the variations of z_0/d and α with the specific gravity s, respectively. The figures show that both z_0 and α increase with a decrease of s. These result seems to be reasonable because the decrease of s results in more intensive movement of the sediment. However, it is noted that the results do not approach the values for fixed beds, $z_0/d = 1/15$ and $\alpha = \sqrt{f/2}/\kappa$, even when s becomes large. That is because the present model assumes the fluid-sediment mixture flow as a continuum, consequently it is not applicable to flow conditions when only a few layers of sediment particles move.

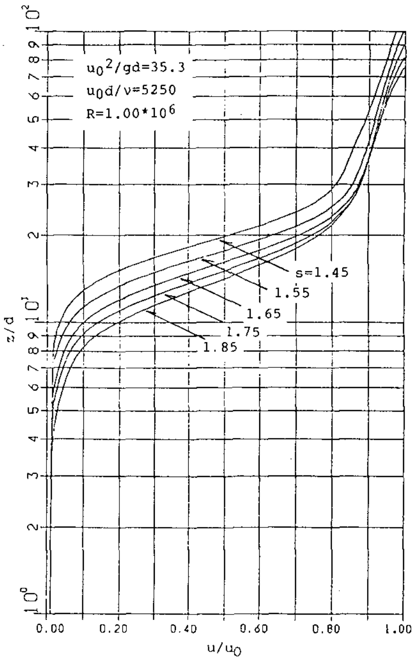

Fig. 6 Semi-log plot of fluid velocity

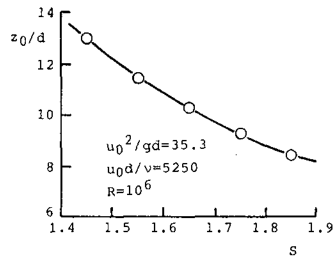

Fig. 7 (a)

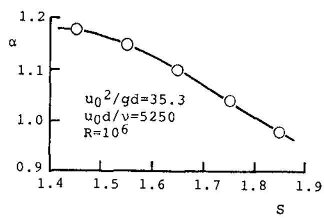

Fig. 7 (b)

Variation of z_0/d and α with specific gravity s

4. COMPARISON WITH EXISTING EXPERIMENTAL DATA

Three sets of data of Ahilan-Sleath(1987), Horikawa et al.(1982) and Yamashita et al.(1985) are used to examine the validity of the present model. All three experiments were carried out in oscillatory tunnels. Horikawa et al. used fine sand, whereas the others used light plastic particles. The experimental conditions are summerized in Tabel-1.

First, comparisons on the sediment transport velocity at phase = 0π between the measurements of Ahilan-Sleath and the predicted results are made as shown in Fig.8. The results of cases (a) and (b) were obtained using nylon particles with a small specific density (s=1.137), while case(c) uses particles of slightly higher density(s =1.44). The calculated velocity for case (c) becomes very small in the region $z \leq 3$ cm. Considering that the location of the immovable layer may not be easily determined in the experiment, the plotted data points are shifted upward by 3cm for this case.

Table 1 Test condition of existing data

		s	T (sec)	u_0 (cm/sec)	d (cm)	R ($*10^5$)	$\frac{u_0^2}{gd}$	$\frac{u_0 d}{\nu}$	$\frac{u_0^2}{(s-1)gd}$
Ahilan-	Test-2	1.137	3.67	45.0	0.40	1.18	5.17	1800	37.7
Sleath	Test-5	1.137	3.59	31.5	0.40	0.57	2.53	1260	18.5
(1987)	Test-9	1.44	4.86	122.0	0.43	11.5	38.0	5246	86.3
Horikawa et al. (1982)	Case 1-1	2.66	3.60	127.0	0.02	9.24	823	254	496.0
Yamashita et al. (1985)	Case-2	1.58	3.10	80.6	0.50	3.21	13.3	4030	22.9

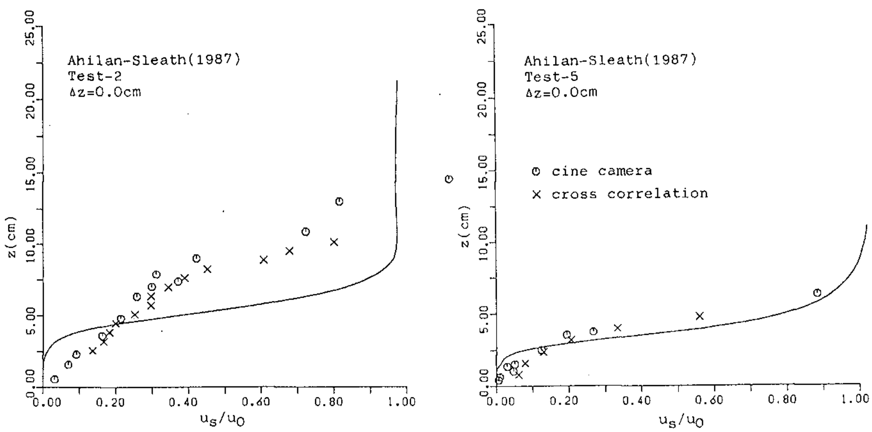

(a) (b)

Fig. 8 Comparison between Ahilan-Sleath(1987)'s data and predicted results on sediment transport velocity

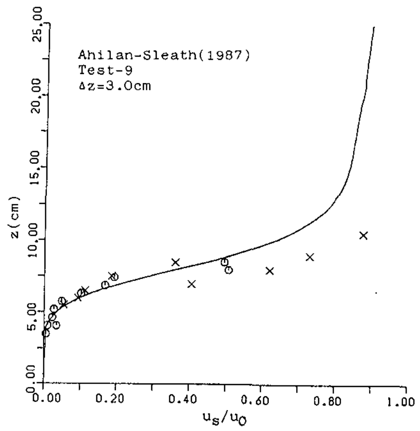

Fig. 8 (c) (conti.)

Second, the data of Yamashita et al. on the fluid velocity and sediment transport velocity are compared. The compared results are shown in Fig.9 for different phases. Although small discrepancies are found, the predicted results are consistant with the following experimental properties: the heights where the velocity starts to increase from 0, the phase precedence of the velocity variation from the free stream velocity, and the decrease of the sediment transport velocity relative to the fluid velocity during the accelerating phase.

Finally, the data of Horikawa et al are examined. The predicted results do not agree well with this data set, because the measured values of u_s and c vary only in a thin region close to the immovable layer. The cause of the discrepancy, which is not obvious however, might be due to the very fine sand particles they used as the sediment.

5. CONCLUSIONS

A mathematical model is developed to describe the flow field under oscillatory sheet flow. The model is based on the conservation of mass and momentum for the fluid and sediment. In order to simplify the model, certain assumptions on the settling velocity, turbulent stress and intergranular stress are introduced. The trend of the calculated results on the concentration, the fluid velocity and the sediment transport velocity are examined. Finally, comparisons with availabled data are made. The conclusions obtained herein are as follows:

(1) In the high concentration region close to the immovable layer, the sediment transport velocity approaches zero due to the intergranular stress, and consequently the fluid velocity becomes small in this region due to the fluid-sediment drag resistance. The phase variation of the velocity in this region is similar to that of a seepage flow. In the low concentration region, the sediment transport velocity becomes smaller than the fluid velocity during the accelerating phase and larger during the decelerating phase.

(2) The changes of the fluid velocity profiles can be described by the gradient and z-intersection of the logarithmic distribution. These two parameters can be described by the four dimensionless parameters involved in the present model.

(3) The present model is capable of predicting most of the experimental data considered here.

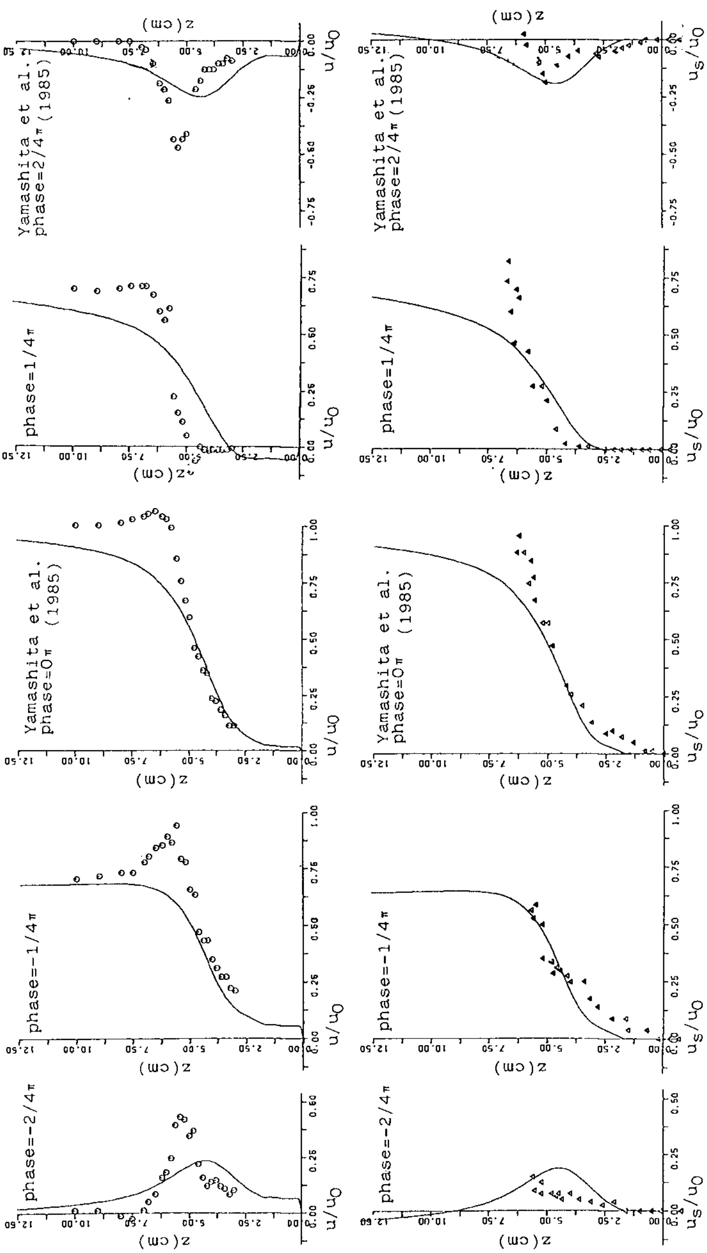

Fig. 9 Comparison between Yamashita et al.(1985)'s data and predicted results on fluid velocity (the upper row) and sediment transport velocity (the lower row).

The present model has tentatively adopted the empirical relationship for the intergranular stress which was originally obtained for a unidirectional flow. There remains the future work of re-examining the assumed distributions for the turbulent eddy viscosity and turbulent diffusion coefficient. Studies on the basic mechanisms involved in a sediment laden oscillatory flow is essential to improve the model accuracy, and accumulation of reliable experimental data is also needed.

ACKNOWLEDGMENTS

Part of this study was carried out at the Institute of Hydrodynamics and Hydraulic Engineering (ISVA), Technical University of Denmark. The staff at ISVA are appreciated for their useful comments and their helpfulness. The author would also like to thank Prof. N. Kobayashi, Delaware University, for constructive comments, and Prof. J. F. A. Sleath, Cambridge University, for sending his useful data.

REFERENCES

Ahilan R. V. and J. F. A. Sleath : Sediment transport in oscillatory flow over flat beds, J. of Hydraulic Engrg. , Vol. 113, NO.3 ,pp.308-322,1987.

Asano T. : Energy dissipation in oscillatory flow over plane movable beds, Progress Report No.68, Inst. of Hydrodyn. and Hydraulic Eng., Technical University of Denmark, pp.3-14, 1988.

Bagnold, R. A. : Experiments on a gravity free dispersion of large solid spheres in a Newtonian fluid under shear, Proc. of Royal Soc. , A225, pp.49-63, 1954.

Bakker, W. T. and W. G. M. van Kesteren : The dynamics of oscillatory sheetflow, Proc. of 20th ICCE, pp.940-954, 1986.

Bogardi, J. : Sediment Transport in Alluvial Streams, Akademiai Kiado, Budapest, Hungary, p.826, 1974.

Brevik I. : Oscillatory rough turbulent boundary layers : Proc. of ASCE, WW3, Vol.107, AUg., pp.175-190, 1981.

Grant, W. D. and O. S. Madsen : Movable bed roughness in unsteady oscillatory flow, J. of Geophy. Res. , Vol. 87, No. c1, pp.469-481, 1982.

Hanes, D. M. and A. J. Bowen : A granular-fluid model for study intense bed-load transport, J. of Geophys. Res., Vol.90, No.C5, pp.9149-9158.

Horikawa, K., A. Watanabe and S. Katori : Sediment transport under sheet flow condition, Proc. of 18th ICCE, pp.1335-1352, 1982.

Kobayashi N. and S. N. Seo : Fluid and sediment interaction over a plane bed, J. of Hydraulic Engrg., ASCE, pp.903-921, 1985.

Richardson J. F. and M. A. daS Jeronimo : Velocity-voidage relations for sedimentation and fluidization, Chem. Eng. Sci., Vol.34, pp.1419-1422, 1979.

Savage, S. B. and S. McKeown : Shear stresses developed during rapid shear of concentrated suspensions of large spherical particles between concentric cylinders , J. Fluid Mech, Vol. 127, pp. 453-472, 1983.

Wilson K. C. : Analysis of contact-load distribution and application to deposit limit in horizontal pipes, J. of Pipelines, Vol.4, pp. 171-176, 1984.

Yamashita T., M. Sawamoto, H. Takeda and G. Yokomori : A study on oscillatory flow and sediment transport at sheet flow condition, Proc. of Japanese Conf. on Coastal Eng., JSCE, pp.297-301, 1985(in Japanese).